Density Functional Calculations of Pd Nanoparticles Using a Plane-Wave Method†

Francesc Viñes,‡ Francesc Illas,*,‡ and Konstantin M. Neyman*,‡,§

Departament de Química Física & Institut de Química Teòrica i Computacional (IQTCUB), Universitat de Barcelona, 08028 Barcelona, Spain, and Institució Catalana de Recerca i Estudis Avançats (ICREA), 08010 Barcelona, Spain

Received: February 19, 2008; Revised Manuscript Received: April 1, 2008

We deal with usage of plane-wave density functional calculations of crystallites formed of 100−200 transition metal atoms to mimic larger experimentally treated particles. A series of model Pd clusters containing up to 225 atoms is chosen as an example. We focused on the description of size-dependent geometric parameters and binding energies of these clusters as compared with previous benchmark calculations; evolution of the particle electronic structure with increasing size has also been addressed. The high performance of the plane-wave calculations for transition-metal nanoparticles has been documented. Implications of this work on broadening opportunities to design and study realistic models of catalytic systems are outlined.

Introduction

Supported transition and noble metal clusters of a few nanometers are ubiquitous in many applications, for example, catalysis.[1] To reduce the complexity of supported metal catalysts, so-called model catalysts have been designed[2] and successfully employed in experimental studies.[3–5] But they are still too complex for accurate description by means of first-principles electronic structure methods. Such calculations of metal particles of 10^3-10^4 atoms commonly exposed in the model catalysts still remain prohibitive.

It was demonstrated, however, that three-dimensional (3D) model metal crystallites cut from the bulk by low-index planes and containing ∼100 atoms allow one to adequately mimic chemical interactions with notably larger metal particles of similar shape.[6–12] Virtues of the 3D cluster models compared to yet more conventional two-dimensional (2D) ones of extended surfaces[13,14] are related to the absence of boundary atoms in a low coordination,[6] inherent in the 2D models. Adequate representation of the reactivity of the metal species in supported metal catalysts requires the sizes of the 3D models, where their properties are scalable to those of the bulk.[15,16] A completely different situation emerges when dealing with the reactivity of smaller (subnanosize) species exhibiting specific size effects where each atom counts. That different nonscalable behavior of smaller clusters, by definition, cannot be predicted on the basis of inter- or extrapolation; such quasi-molecular effects are expected for 3D clusters of up to ∼50 Pd atoms.[6]

Up to now, density functional (DF) studies of size-converged 3D models of metal particles in catalytic systems[6–12] have only been performed with the help of a powerful code for molecular parallel calculations, ParaGauss.[17,18] These accurate scalar relativistic all-electron calculations of metal particles with a diameter of 1−2 nm, which contain 100 and more atoms, required to impose point-group symmetry constraints to reduce the computational demand. Feasibility of large-scale calculations for adsorption and reactions on the cuboctahedral model Pd_{79} has also recently been demonstrated by using relatively low point-group symmetry D_4.[12] This reduced-symmetry approach enabled deposition of adsorbates without any local restrictions on cluster facets and edges. Thus, it opened a way to study reaction pathways on both regular and defect sites of the same large enough nanoparticle.

Nevertheless, models without any symmetry restrictions may become essential in several practically relevant cases. One can think, for instance, of a very low surface coverage[11] or reactivity of bi- and polymetallic crystallites of arbitrary structural ordering or without any ordering at all;[9] moreover, explicit consideration of the supporting material may be mandatory. Complete release of the symmetry constraints imposed on metal nanoparticle substrates of ∼100 atoms would make their accurate DF treatment by using the molecular cluster scheme[6] hardly possible. An alternative is to use the computational technology offered by the methods employing plane-wave basis sets (and therefore periodic boundary conditions), such as Vienna ab initio simulation package (VASP).[19–21] A prerequisite is that the computational cost and accuracy for moderately large metal nanoparticles are comparable to those of the molecular approach.[6–12] Indications that this is the case have recently been published (see, e.g., refs 22 and 23). However, no assessment of the applicability of such plane-wave strategy to model large metal nanoparticles in catalysis has been communicated so far.

In this work, we report a systematic study on the performance and practicability of VASP calculations of 3D crystallites with 100−200 atoms, ultimately to describe particles in metal catalysts without symmetry restrictions. For this purpose, a series of (cub-)octahedral clusters Pd_n, containing up to 225 atoms, has been designed, and their atomic and electronic structure has been calculated. In particular, we focused on the description of size-dependent properties. We demonstrated that the electronic structure of these nanoparticles, analyzed in terms of density of states (DOS) parameters, evolved with increasing size in a rather straightforward fashion to that of Pd bulk. Calculated average interatomic distances and cohesive energies of the nanoparticles are found to scale with size to the corresponding bulk values with a high precision similar to that in the previous benchmark all-electron scalar relativistic calculations.[6,15,26] Thus,

† Part of the special section for the "Symposium on Energetics and Dynamics of Molecules, Solids and Surfaces".

* Corresponding authors. E-mail: francesc.illas@ub.edu and konstantin.neyman@icrea.es.

‡ Universitat de Barcelona.

§ Institució Catalana de Recerca i Estudis Avançats.

10.1021/jp8014854 CCC: $40.75
Published on Web 06/06/2008

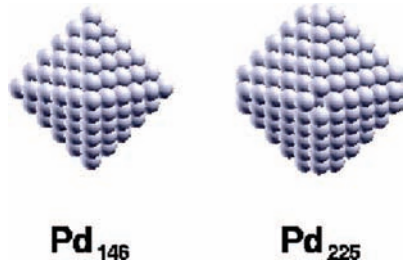

Figure 1. Sketches of the example clusters studied, Pd_{146} and Pd_{225}.

the efficiency of VASP calculations is concluded to be sufficient also for large-scale reactivity studies of 3D model metal particles of relevance for catalysis.

Computational Details and Models

DF calculations using a plane-wave basis set have been carried out by using the VASP code.[19–21] The interaction between the atomic cores and valence electrons was described by the projector augmented wave (PAW) method.[24,25] We compared a scheme in which Pd 4p electrons were assigned to core electrons (thereafter, Pd_{C4p}), with one where Pd 4p electrons belong to the explicitly treated valence shell (Pd_{V4p}). After extensive benchmarking, a cutoff of 250 eV in the kinetic energy proved to be sufficiently accurate for the present study. This has been established by comparing the total energy for the Pd_{38} cluster by using 230, 250, and 270 eV cutoff values. The difference in total energy for the two largest cutoff thresholds is ~0.01 eV only, whereas this difference becomes ~0.6 eV when comparing values obtained by using the two smallest cutoff values. A Gaussian smearing technique (broadening width 0.2 eV) was applied to enhance convergence; but finally, all energies were extrapolated to zero smearing (at 0 K); DOS plots were calculated with a smaller broadening width, 0.05 eV. According to previous scalar relativistic cluster DF studies of Pd nanoparticles,[6,15,26] most accurate geometric parameters are provided by local density approximation (LDA), whereas calculations using generalized gradient approximation (GGA) deliver more precise energies. The lack of a sufficiently accurate universal exchange-correlation functional prompted us to use the following combined approach, justified elsewhere:[6,10] geometry optimization was performed throughout at an LDA level by using the Vosko−Wilk−Nusair (VWN) functional;[27] after that, GGA energies were calculated in a single-point fashion by using the Perdew−Wang (PW91) functional.[28] The present calculations use large periodically repeated unit cells to describe discrete clusters. Therefore, only the Γ point of the reciprocal space was used. The center of each nanoparticle was located in the origin of the unit cell. To avoid interactions between the Pd_n particles in the periodically repeated structures, the particles were kept at least 1 nm apart from each other. In fact, the unit cell for all clusters was the same and was defined by the largest studied cluster (Pd_{225}) with 1 nm of vacuum in each direction. According to our tests, interparticle interactions start at distances of ~0.4 nm.[23] To provide reference data (see below), calculations for Pd bulk have been performed; here, a unit cell comprised of four atoms and a Monkhorst−Pack k point grid $13 \times 13 \times 13$ were used.

We studied the following series of model (cub-)octahedral crystallites: Pd_{38}, Pd_{44}, Pd_{55}, Pd_{79}, Pd_{85}, Pd_{116}, Pd_{140}, Pd_{146}, and Pd_{225}, which contains all benchmark systems calculated at scalar relativistic DF cluster level,[6] to enable a direct comparison. Each of the above particles is a subsystem of the largest moieties sketched in Figure 1, either of Pd_{146} or of Pd_{225} (~1.9 nm diameter each). Particles Pd_{55}, Pd_{79}, Pd_{85}, and Pd_{225} are constructed by successive deposition of complete or vertex-truncated octahedral shells of Pd atoms around a central one. Another set, Pd_{38}, Pd_{44}, Pd_{116}, Pd_{140}, and Pd_{146}, originates from consecutive (symmetrical) atom assembly around the Pd_6 core.

Initial cluster geometries with slightly distorted atomic positions with respect to Pd bulk were used with the nearest Pd−Pd distances experimentally determined to be 275.1 pm.[29] No symmetry constraint was applied in the course of complete geometry optimization of the Pd crystallites to the corresponding local minima. Nevertheless, all resulting structures were found to be symmetric to within at least 1 pm in the atomic positions. The remaining forces acting on each atom in the optimized geometries were always smaller than 0.2 eV/nm. According to our tests, geometric parameters calculated by using larger core Pd_{C4p} and smaller core Pd_{V4p} PAW variants (see above) are essentially equal. A rather small constant offset of the cohesive energies per atom, $\Delta E_b/n \approx 9$ kJ mol^{-1} (stronger binding), obtained in the Pd_{C4p} scheme compared to the Pd_{V4p} one, justified usage of the more economic (by ~30%) Pd_{C4p} approach as a standard. The computer time required for geometry optimization (usually 15−25 geometry cycles suffice) of the clusters up to Pd_{140} (8 Intel Xeon 2.8 GHz processors of 32 bits ordered in 4 nodes with 2 processors each) depends almost linearly on the number of atoms in the cluster and is 16−20 min/atom. Calculations showed basically linear scaling with the number of processors up to 32 processors. For the largest particle, Pd_{225}, computational demand became quite severe, and calculations had to be carried out in a large parallel supercomputer.

Although some small Pd clusters exhibit an open-shell electronic ground state,[30,31] spin polarization effects in moderately large particles (~80 atoms and onward) resulted in a very small change in the cohesive energy, which became really negligible for somewhat larger particles (Pd_{140}).[31] This is in line with previous results[11] and also with our test calculations. For instance, for the Pd_{79} particle, a spin polarized solution has been found at the LDA and GGA levels, but the total energy is only 0.007 and 0.1 eV, respectively, lower than the one corresponding to the closed-shell solution. In addition, spin polarization does not introduce any change in the geometric structure; the Pd_{79} structure optimized at the LDA or GGA level remains unchanged when spin polarization is explicitly taken into account. Therefore, all calculations discussed in the following have been carried out without the spin polarization. Note in addition that spin polarization effects are smaller than those introduced by the variation of an exchange-correlation potential.

Results and Discussion

Selected calculated structural and energetic observables of the cluster series Pd_{38}−Pd_{225} are collected in Table I and compared with calculated and experimental results for Pd bulk. The following two parameters (not affected by the geometry optimization) are useful to characterize the surface/bulk features of the Pd_n nanocrystallites under scrutiny: the average coordination number N_{av}, defined as the sum of the coordination numbers of all n atoms of a cluster divided by n, and the fraction of surface atoms, n_s/n. These two indicators clearly manifest development of bulk character along the series with increasing n. They also reveal that even the largest nanocrystallite considered, Pd_{225}, with its 62% of surface atoms and N_{av} more than 20% smaller than $N_{av} = 12$ in the bulk, is still quite far from the bulk limit. It is interesting to quantify how the structure and energetic of the crystallites approach the values of bulk material with growing size and to compare the results with available benchmark data.

TABLE I: Calculated Average (d), Minimum (r_{min}), and Maximum (r_{max}) Nearest Pd−Pd Distances (pm) between Different Types of Atoms of Pd_n Crystallites and Binding Energy per Atom, E_b/n (kJ mol^{-1}), in Comparison with Pd Bulk Data

parameter	Pd_{38}	Pd_{44}	Pd_{55}	Pd_{79}	Pd_{85}	Pd_{116}	Pd_{140}	Pd_{146}	Pd_{225}	Bulk
N_{av}[a]	7.58	7.64	7.85	8.51	8.47	8.90	9.09	9.04	9.49	12.0
n_s/n[b]	0.84	0.86	0.76	0.76	0.78	0.67	0.69	0.70	0.62	0.00
d_{OS}[c]	264	263	265	265	265	266	265	265	268	
$r_{min,OS}$[c]	264	254	263	262	258	263	260	258	262	
$r_{max,OS}$[c]	264	270	273	268	273	270	269	272	280	
d[d]	266	266	266	268	268	268	269	269	269	273, 275[e]
r_{min}[d]	263	254	261	262	258	260	260	258	262	
r_{max}[d]	276	285	275	279	280	276	280	281	280	
E_b(VWN)/n[f]	366 (357)	371 (360)	376 (369)	393 (386)	394 (386)	404 (398)	410 (404)	409 (403)	422 (416)	485 (483)
E_b(PW91)/n	266	270	275	287	287	294	299	299	308	358, 377[g]

[a] Average coordination numbers. [b] Number of surface atoms n_s. [c] Nearest Pd−Pd distances between the outer-shell (OS) atoms to which all surface atoms belong. [d] Nearest Pd−Pd distances overall. [e] Experiment (ref 29). [f] In parentheses, E_b(VWN)/n computed with r(Pd−Pd) fixed at the experimental distance of Pd bulk. [g] Experiment (ref 33).

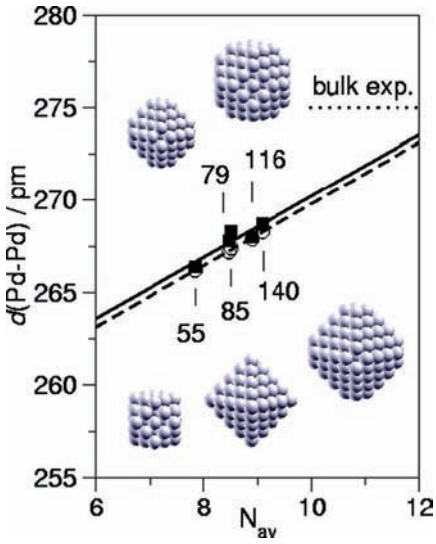

Figure 2. Average nearest distances d(Pd−Pd) of bare Pd nanoparticles, Pd_{55}−Pd_{140}, optimized at LDA(VWN) level as a function of the average coordination number, N_{av}. Solid line (filled squares) represents plane-wave calculations: fitted correlation (in pm) d(Pd−Pd) = 253.6 + 1.661N_{av}; value extrapolated to Pd bulk is 273.5 pm, and that optimized for Pd bulk is 272.7 pm. Dashed line (open circles) represents scalar relativistic cluster calculations using O_h point-group symmetry (ref 6): fitted correlation (in pm) d(Pd−Pd) = 253.1 + 1.667N_{av}; value extrapolated to Pd bulk is 273.1 pm.

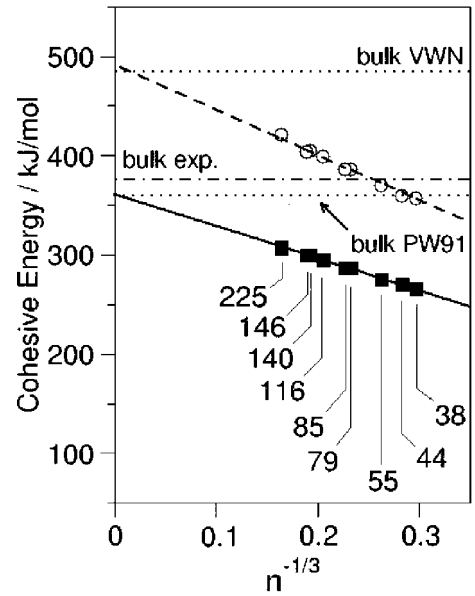

Figure 3. Average cohesive energy per atom, E_b/n, of bare nanoparticles Pd_{38}−Pd_{225} predicted by plane-wave calculations as a function of the inverse of the mean particle radius, $R^{-1} \approx n^{-1/3}$. Solid line (filled squares), E_b(PW91)/n; dashed line (open circles), E_b(VWN)/n. Fitted correlations (in kJ mol^{-1}): E_b(PW91)/n = 359.0 − 313.9$n^{-1/3}$ (R^2 = 0.997) and E_b(VWN)/n = 490.9 − 425.1$n^{-1/3}$ (R^2 = 0.996). Also shown are the bulk values calculated at PW91 and VWN levels, 358 and 485 kJ mol^{-1}, respectively, and the experimental cohesive energy of Pd bulk, 377 kJ mol^{-1} (ref 33).

Optimized nearest-neighbor interatomic Pd−Pd distances can be characterized by average values d as well as by maximum, r_{max}, and minimum, r_{min}, values, both for all Pd atoms in the particles and for only the least-coordinated outer-shell (OS) part of them. In the particle size range studied (Table I), d and d_{OS} values remain noticeably smaller than those of the bulk reference and vary by essentially the same magnitude, 3−4 pm, exhibiting a clear bond-elongation trend for larger species.[6,15,26] The Pd−Pd distances on the particle surface, d_{OS}, are always shorter than those in the inner part. The difference $r_{max} - r_{min}$ = 31 pm calculated for the Pd_{44} moiety is the largest one over the whole set of particles, thus reflecting the strongest distortion of Pd_{44}. (Note that this cluster size still most probably belongs to the nonscalable region, see Introduction). In general, the deviation of the largest/smallest Pd−Pd bond lengths of each cluster from the corresponding d values is only slightly affected by the octahedral symmetry imposed. For instance, for the rather large Pd_{140} species, the range r_{max}− r_{min} is within $d \pm 10$ pm in the present study, compared with $d \pm 6$ pm calculated under O_h symmetry constraint.[6]

In Figure 2, we compare scaling of the average Pd−Pd bond distance d with the cluster size (expressed in terms of the average coordination number, N_{av}) as calculated at the VWN level in the present approach with the scaling quantified in a previous work employing point-group models.[6] Based on the present estimation for Pd_{55} moiety and on earlier data,[15,26] geometry optimization at a GGA level would result in ∼8 pm larger d(Pd−Pd) values. For a direct comparison,[32] we included in the correlation data of the same species Pd_{55}, Pd_{79}, Pd_{85}, Pd_{116}, and Pd_{140} as in ref 6. The present fitted correlation (in pm) d = 253.6 + 1.661N_{av} gives a value extrapolated to Pd bulk of 273.5 pm, very close to 272.7 pm, which we explicitly calculated for Pd bulk (Table I). These data are in very good agreement with the results of scalar relativistic cluster calculations performed using O_h point-group symmetry. There, the fitted correlation was d = 253.1 + 1.667N_{av}, and the distance extrapolated to Pd bulk was 273.1 pm.[6]

One can use the correlations to predict deviations of the average distance d from that extrapolated to the bulk for particles

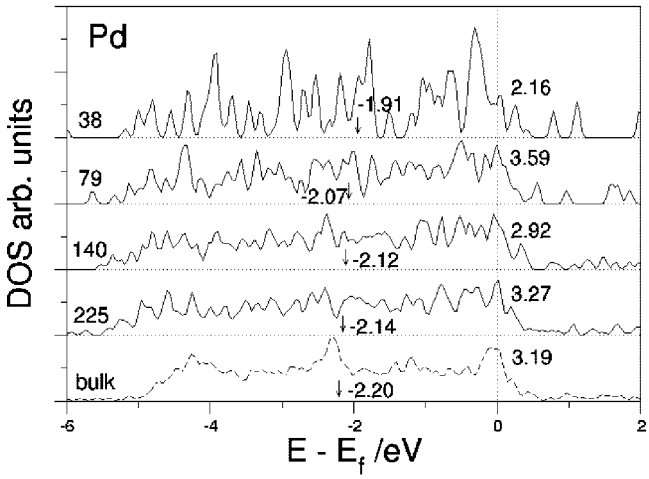

Figure 4. GGA DOS plots calculated with a Gaussian smearing of 0.05 eV for selected nanoparticles Pd_n of increasing size (n = 38, 79, 140, 225; solid lines) compared to the corresponding plot of bulk Pd (dashed line). Arrows and numbers near them indicate centers of the valence d bands. DOS values per atom at the Fermi level E_f are also given.

notably larger than those that could be treated computationally. For the octahedral cluster Pd_{1834}, the estimation results in a d value which is still 2 pm shorter than that extrapolated to the bulk. Only for such a large cuboctahedral Pd_{8217} moiety would one match the extrapolated to bulk estimate within ~1 pm.

The average cohesive energy per atom, E_b/n, is another important characteristic of Pd_n nanoparticles. E_b/n can be extrapolated to the bulk value as a function of the inverse of the mean particle radius R,[6,15,26] approximated as $R^{-1} \approx n^{-1/3}$. Results of such extrapolation of the LDA(VWN) and GGA(PW91) cohesive energies E_b/n calculated for the whole range of Pd_n clusters, $38 \leq n \leq 225$, are shown in Figure 3. Fitted correlations (in kJ mol^{-1}) $E_b(PW91)/n = 359.0 - 313.9n^{-1/3}$ ($R^2 = 0.997$) and $E_b(VWN)/n = 490.9 - 425.1n^{-1/3}$ ($R^2 = 0.996$) are essentially perfectly linear. The extrapolated to the bulk PW91 and VWN values agree quantitatively with the corresponding bulk values calculated explicitly, 358 and 485 kJ mol^{-1}. Importantly, the latter bulk values are completely consistent internal references obtained by using exactly the same computational procedure as the individual cluster values. One should mention that the $E_b(PW91)/n$ bulk values are only slightly smaller than the experimental cohesive energy of Pd bulk, 377 kJ mol^{-1};[33] as is usual for LDA energies, the $E_b(VWN)/n$ value considerably overestimates the experimental one. Another observation is that starting from the cluster Pd_{55} and onward, the calculated E_b/n energy for the crystallites with all r(Pd−Pd) fixed at the bulk value (Table I, in parentheses) deviates from the energy of the corresponding optimized species by only 1−2%, in line with previous results.[6,26]

Beyond the difference in imposing or not symmetry constraints on the model nanoparticles in the previous single-particle (cluster) and present calculations, these two computational methodologies exhibit other significant distinctions, such as all-electron scalar relativistic calculations with Gaussian-type orbitals (GTO) versus PAW calculations with a plane-wave strategy. Despite that, the energy correlations obtained in the cluster work,[6] $E_b(BP86)/n = 355 - 332n^{-1/3}$ ($R^2 = 0.993$) and $E_b(VWN)/n = 506 - 481n^{-1/3}$ ($R^2 = 0.993$) as well as the bulk extrapolated E_b/n values match the corresponding present data with an absolute accuracy better than 15 kJ mol^{-1}. It is a clear evidence of the high enough precision of the PAW approach, which together with the computational efficiency of the latter also justifies energy studies of moderately large 4d metal nanoparticles without any symmetry constraint.

Finally, we comment on the size dependence of the electronic structure of the nanoparticles and on how it approaches the electronic structure of the bulk Pd. We analyze the electronic structure in terms of the DOS. Peculiarities of DOS are responsible for differences in the reactivity and thus could have important implications for catalysis.[34] Another aspect of general interest is how the bulk-like electronic properties are developed for metal nanoparticles when their size is increasing. In other words, the issue of interest is at which size range the particles start to behave not as large molecules with discrete electronic levels but as the smallest metallic pieces of bulk.

In Figure 4, GGA DOS plots for selected nanoparticles Pd_n of increasing size (n = 38, 79, 140, 225) are compared to each other and to the plot for the bulk metal. Molecular character of Pd_{38} is clearly seen, for instance, from numerous regions of the zero DOS amplitude. In general, Figure 4 shows the fast evolution of the DOS toward the bulk Pd with increasing particle size. An important question is at which size the particles become sufficiently large, so that their DOS parameters monotonously approach those of the bulk. As an indicator of the DOS evolution with particle size, we have chosen positions of the center of valence d band,[34] corresponding to the half of the cumulative d-projected density of states integrated up to the Fermi level (see vertical arrows and numbers near them in Figure 4). For Pd_n starting from Pd_{79}, this indicator monotonously and quite rapidly approaches the bulk value with increasing n. On the other hand, the d-band center for the molecular Pd_{38} species differs notably, by ~0.2 eV, from that of larger particles. Furthermore, the d-band center for the Pd_{55} species (DOS not shown in Figure 4), −1.83 eV, which is more positive than the value of −1.91 eV calculated for the smaller Pd_{38} moiety, indicates that the onset of scalable-to-bulk properties for Pd nanoparticles (here, based on evolution of DOS parameters) requires about 80 atoms, exactly as what has been found on the basis of the evolution of the adsorption properties.[6] Finally, DOS values per metal atom calculated for Pd_n species at the Fermi level E_f, also presented in Figure 4, provide further evidence for the rather close similarity of the electronic structure of Pd_{140} and Pd_{225} particles with the bulk Pd, as well as for noticeable differences with the electronic structure of Pd_{38}. However, this indicator of the electronic structure alteration appears to be less characteristic than the center of the d band.

Summary and Conclusions

We assessed applicability of plane-wave DF calculations to model clusters comprised of about 100 transition-metal atoms, which have been previously shown to accurately represent adsorption properties and reactivity of notably larger metal particles present in supported metal catalysts. To this end, calculations have been carried out for a series of nine octahedral and cuboctahedral Pd_n crystallites cut from Pd bulk, with a nuclearity n up to 225. We described the structure of and the bonding in these nanoparticles, focusing on the scalability of these properties to those of Pd bulk, and also compared those results to previous benchmark all-electron scalar relativistic calculations that use GTO basis sets. The computational feasibility and high accuracy of this plane-wave DF approach open an attractive way to widely employ compact moderately large crystallites as realistic models in high-level electronic structure studies of catalysts and chemical reactions on them,[8,12] without a need of local symmetry restrictions. Models with no

local symmetry imposed may become crucial, for instance, when very low surface coverage of rather strongly adsorbed reactant/product species is considered, when nanoparticles do not exhibit sufficient structural ordering (as is often the case for catalysts made of more than one metal component), or when explicit consideration of the supporting material is required.

The strategy of plane-wave calculations of metal nanoparticles addressed in the present study is used in our ongoing investigations of adsorption properties and reactivity of catalytic systems. We anticipate that such modeling approach will very soon become state of the art in this research area.

Acknowledgment. F.V. thanks the Spanish Ministry of Education and Science (MEC) and Universitat de Barcelona for supporting his predoctoral research. Financial support has been provided by the MEC (Grants CTQ2005-08459-CO2-01, UNBA05-33-001, and HA2006-0102) and the Generalitat de Catalunya (Grants 2005SGR00697 and 2005 PEIR 0051/69). Computational time on the *MARENOSTRUM* supercomputer of the Barcelona Supercomputing Center is gratefully acknowledged.

References and Notes

(1) *Chemisorption and Reactivity on Supported Clusters and Thin Films. Towards an Understanding of Microscopic Processes in Catalysis, NATO ASI Series*; Lambert, R. M., Pacchioni, G., Eds.; Kluwer Academic Publishers: Dordrecht, The Netherlands, 1997; pp 1−532.

(2) Bäumer, M.; Freund, H.-J. *Prog. Surf. Sci.* **1999**, *61*, 127–198.

(3) Dellwig, T.; Rupprechter, G.; Unterhalt, H.; Freund, H.-J. *Phys. Rev. Lett.* **2000**, *85*, 776–779.

(4) Schauermann, S.; Hoffmann, J.; Johánek, V.; Hartmann, J.; Libuda, J.; Freund, H.-J. *Angew. Chem., Int. Ed.* **2002**, *41*, 2532–2535.

(5) Morkel, M.; Kaichev, V. V.; Rupprechter, G.; Freund, H.-J.; Prosvirin, I. P.; Bukhtiyarov, V. I. *J. Phys. Chem. B* **2004**, *108*, 12955–12961.

(6) Yudanov, I. V.; Sahnoun, R.; Neyman, K. M.; Rösch, N. *J. Chem. Phys.* **2002**, *117*, 9887–9896.

(7) Yudanov, I. V.; Sahnoun, R.; Neyman, K. M.; Rösch, N.; Hoffmann, J.; Schauermann, S.; Johánek, V.; Unterhalt, H.; Rupprechter, G.; Libuda, J.; Freund, H.-J. *J. Phys. Chem. B* **2003**, *107*, 255–264.

(8) Yudanov, I. V.; Neyman, K. M.; Rösch, N. *Phys. Chem. Chem. Phys.* **2004**, *6*, 116–123.

(9) Neyman, K. M.; Sahnoun, R.; Inntam, C.; Hengrasmee, S.; Rösch, N. *J. Phys. Chem. B* **2004**, *108*, 5424–5430.

(10) Neyman, K. M.; Vayssilov, G. N.; Rösch, N. *J. Organomet. Chem.* **2004**, *689*, 4384–4394.

(11) Neyman, K. M.; Inntam, C.; Gordienko, A. B.; Yudanov, I. V.; Rösch, N. *J. Chem. Phys.* **2005**, *122*, 174705.

(12) Yudanov, I. V.; Neyman, K. M.; Rösch, N. *Phys. Chem. Chem. Phys.* **2006**, *8*, 2396–2401.

(13) Whitten, J. L.; Yang, H. *Surf. Sci. Rep.* **1996**, *24*, 55–124.

(14) Neyman, K. M.; Illas, F. *Catal. Today* **2005**, *105*, 2–16.

(15) Krüger, S.; Vent, S.; Rösch, N. *Ber. Bunsenges. Phys. Chem.* **1997**, *101*, 1640–1643.

(16) Baletto, F.; Ferrando, R. *Rev. Mod. Phys.* **2005**, *77*, 371–423.

(17) Belling, T.; Grauschopf, T.; Krüger, S.; Mayer, M.; Nörtemann, F.; Staufer, M.; Zenger, C.; Rösch, N. Quantum chemistry on parallel computers: Concepts and results of a density functional method. In *High Performance Scientific and Engineering Computing. Lecture Notes in Computational Science and Engineering*; Bungartz, H.-J., Durst, F., Zenger, C., Eds.;Springer: Heidelberg, Germany, 1999; Vol. 8, pp 441−455.

(18) Belling, T.; Grauschopf, T.; Krüger, S.; Nörtemann, F.; Staufer, M.; Mayer, M.; Nasluzov, V. A.; Birkenheuer, U.; Hu, A.; Matveev, A. V.; Shor, A. M.; Fuchs-Rohr, M. S. K.; Neyman, K. M.; Ganyushin, D. I.; Kerdcharoen, T.; Woiterski, A.; Gordienko, A. B.; Majumder, S.; Rösch, N. *ParaGauss*, Version 3.0. TU München: München, Germany, 2004.

(19) Kresse, G.; Furthmüller, J. *Phys. Rev. B* **1996**, *54*, 11169–11186.

(20) Kresse, G.; Hafner, J. *Phys. Rev. B* **1993**, *47*, 558–561.

(21) Kresse, G.; Furthmüller, J. *Comput. Mater. Sci.* **1996**, *6*, 15–50.

(22) Barnard, A. S.; Curtiss, L. A. *ChemPhysChem* **2006**, *7*, 1544–1553.

(23) Viñes, F.; Illas, F.; Neyman, K. M. *Angew. Chem., Int. Ed.* **2007**, *46*, 7094–7097.

(24) Blöchl, P. E. *Phys. Rev. B* **1994**, *50*, 17953–17979.

(25) Kresse, G.; Joubert, D. *Phys. Rev. B* **1999**, *59*, 1758–1775.

(26) Krüger, S.; Vent, S.; Nörtemann, F.; Staufer, M.; Rösch, N. *J. Chem. Phys.* **2001**, *115*, 2082–2087.

(27) Vosko, S. H.; Wilk, L.; Nusair, M. *Can. J. Phys.* **1980**, *58*, 1200–1211.

(28) Perdew, J. P.; Wang, Y. *Phys. Rev. B* **1992**, *45*, 13244–13249.

(29) *CRC Handbook of Chemistry and Physics*, 87th ed.; Lide, D. R., Ed.; CRC Press: Boca Raton, FL, 2006−2007; pp 12−17.

(30) Moseler, M.; Häkkinen, H.; Barnett, R. N.; Landman, U. *Phys. Rev. Lett.* **2001**, *86*, 2545–2548.

(31) Nava, P.; Sierka, M.; Ahlrichs, R. *Phys. Chem. Chem. Phys.* **2003**, *5*, 3372–3381.

(32) *For all* clusters considered, $Pd_{38}-Pd_{225}$, the correlation is (pm) $d(Pd-Pd) = 253.6 + 1.658N_{av}$ ($R^2 = 0.936$), and the distance extrapolated to Pd bulk is 273.4 pm. Thus, the uncertainty of the extrapolations due to inclusion of more data is <1 pm.

(33) Wagman, D. D. The NBS Tables of Chemical Thermodynamic Properties. *J. Phys. Chem. Ref. Data* 1982, Vol. 11, Suppl. 2.

(34) Hammer, B.; Nørskov, J. K. *Adv. Catal.* **2000**, *45*, 71–129.

JP8014854